

## Measurement of the Proton-Air Cross Section with Telescope Arrays Black Rock, Long Ridge, and Surface Array in Hybrid Mode.

Rasha Abbasi<sup>a,\*</sup> and William Hanlon<sup>b</sup> on behalf of the Telescope Array Collaboration  
(a complete list of authors can be found at the end of the proceedings)

<sup>a</sup>Department of Physics, Loyola University Chicago, Chicago, U.S.A.

<sup>b</sup>The Smithsonian Astrophysical Observatory

E-mail: [rabbasi@luc.edu](mailto:rabbasi@luc.edu)

Ultra High Energy Cosmic Ray (UHECR) detectors have been reporting on the proton-air cross section measurement beyond the capability of particle accelerators since 1984. The knowledge of this fundamental particle property is vital for our understanding of high energy particle interactions and could possibly hold the key to new physics. The data used in this work was collected over eight years using the hybrid events of Black Rock (BR) and Long Ridge (LR) fluorescence detectors as well as the Telescope Array Surface Detector (TASD). The proton-air cross section is determined at  $\sqrt{s} = 73$  TeV by fitting the exponential tail of the  $X_{max}$  distribution of these events. The proton-air cross section is then inferred from the exponential tail fit and from the most updated high energy interaction models.  $\sigma_{p-air}^{inel}$  is observed to be  $520.1 \pm 35.8$  [Stat.]  $^{+25.3}_{-42.9}$  [Sys.] mb. This is the second proton-air cross section work reported by the Telescope Array collaboration.

37<sup>th</sup> International Cosmic Ray Conference (ICRC 2021)  
July 12th – 23rd, 2021  
Online – Berlin, Germany

<sup>1</sup>(a complete list of authors can be found at the end of the proceedings)

\*Presenter

## 1. Introduction

Ultra High Energy Cosmic Ray (UHECR) detectors have been reporting on the proton-air cross section measurement beyond the capability of particle accelerators since 1984 [4–6, 9, 10, 20, 23, 27]. UHECRs offer a unique opportunity as testing grounds for physics beyond the standard model, as they represent a class of particles in the energy frontier beyond what can be generated in human-made accelerators. UHECRs provide a way to measure the proton interaction cross section at energies beyond those that can be achieved in the lab to test standard model predictions of how the cross section evolves with energy.

The knowledge of this fundamental particle property is vital for our understanding of high energy particle interactions and could possibly hold the key to new physics. This work presents the second Telescope Array report on the proton-air cross section [3]. The first result was reported in 2015 using the Middle Drum (MD) fluorescence detector and the surface detector in hybrid mode [1]. In this proceeding, we are reporting on the inelastic proton-air cross section, at  $\sqrt{s} = 73$  TeV, using eight years of data observed by Black Rock Mesa (BRM) and Long Ridge (LR) fluorescence detectors (FDs) and the surface detector (SD) in hybrid mode.

While more UHECR events have been observed by the Telescope Array detector since the first report, the BRM and LR detectors used in this analysis, are closer in distance to the Surface Detector (SD) array as shown in Figure 1. This enables us to study the inelastic proton-air cross section with higher statistical power for lower energy events.

The technique used to analyze these events is similar to that used in the first proton-air cross section report [1] (the  $K$ -Factor method). The statistical power, on other hand, increased by a factor of four. Note that, all the systematic sources are revisited and updated, in addition to using the latest hadronic models QGSJETII.4 [24], QGSJET01 [21], SIBYLL2.3 [17], and EPOS-LHC [26].

The proton-proton cross section is also calculated in this work using Glauber formalism [18] and BHS fit [12]. The new inelastic proton-air and the total proton-proton cross section results are compared with the previous experimental results and with the predictions of the models.

## 2. Data Analysis

The analysis to obtain the proton-air inelastic cross section ( $\sigma_{p\text{-air}}^{\text{inel}}$ ) is divided into two parts. The first part is the calculation of the value of the attenuation length ( $\Lambda_m$ ) of the observed UHECR events. In the second part, we calculate the inelastic proton-air inelastic cross section ( $\sigma_{p\text{-air}}^{\text{inel}}$ ) value from the obtained attenuation length  $\Lambda_m$ .

### 2.1 Measuring the Attenuation Length $\Lambda_m$

Ideally, observation of the distribution of the amount of material ( $X_1$ ), penetrated by the shower before the first interaction would allow estimating the proton-air cross section directly. However,  $X_1$  is not a direct observable. Therefore, UHECR detectors have been reporting on the proton-air cross section using the slant depth at the shower maximum referred to as  $X_{max}$ .

The value of attenuation length  $\Lambda_m$ , and therefore the proton-air cross section, can be calculated by fitting the  $X_{max}$  distribution tail to the exponential function  $e^{-\frac{X_{max}}{\Lambda_m}}$ . Here only the tail of the  $X_{max}$  distribution is used to obtain  $\Lambda_m$ , because it is the most penetrating part of the distribution

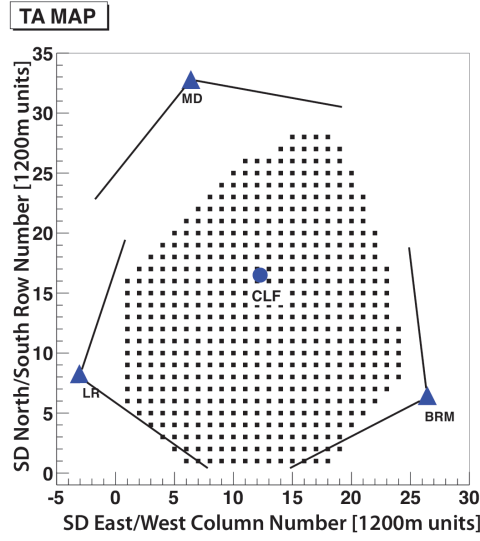


**Figure 1:** The Telescope Array detector configuration. The filled squares are the 507 SD scintillators on a 1.2 km grid. The SD scintillators are enclosed by three fluorescent detectors shown in filled triangles together with their field of view in solid lines. The northernmost fluorescence detector is called Middle Drum while the southern fluorescence detectors are referred to as Black Rock Mesa and Long Ridge. The filled circle in the middle equally spaced from the three fluorescence detectors is the Central Laser Facility used for atmospheric monitoring and detector calibration.

and is assumed to comprise of mostly protons. The choice of the of the fit range for the exponential fit is made to maximize the number of events in the tail distribution while minimizing instability in the value of  $\Lambda_m$  due to possible detector bias or helium contamination. The exponential fit to the slope is done using the unbinned likelihood method between 790 and 1000 g/cm<sup>2</sup>.

Figure 2 shows the  $X_{max}$  distribution of the of the hybrid event data collected by the Telescope Array southernmost fluorescence detectors Black Rock Mesa (BRM) and Long Ridge (LR) and the surface detector (SD). The distribution includes 1975 events in the energy range between  $10^{18.2}$  and  $10^{19}$  eV with an average energy of  $10^{18.45}$  eV.

Several systematic checks are applied to test for the stability of the measured attenuation length  $\Lambda_m$ . This is done by dividing the data in two halves based on: the zenith angle, the distance of the shower using the impact parameter  $R_p$ , and the energy of the event. The subsets divided are found to be consistent within the statistical fluctuations.

Moreover, the systematic effect of possible energy dependent bias in the  $X_{max}$  distribution was studied. This is done by shifting the values of  $X_{max}$  by their elongation rate prior to fitting. The systematic effect from a possible energy bias in the value of  $\Lambda_m$  was found to be negligible.

Systematic effects due to detector bias is tested by comparing the attenuation length calculated with and without detector effects. First, the attenuation length  $\Lambda_m$  is calculated from CONEX simulations, where the detector effect is not included. After which,  $\Lambda_m$  is calculated from CORSIKA simulation, where the events are propagated through the detector, reconstructed, and the quality cuts applied. The systematic error from the difference in  $\Lambda_m$  was found to be consistent within the statistical fluctuations.

The final  $\Lambda_m$  reported by the Telescope Array detector at an average energy of  $10^{18.45}$  eV

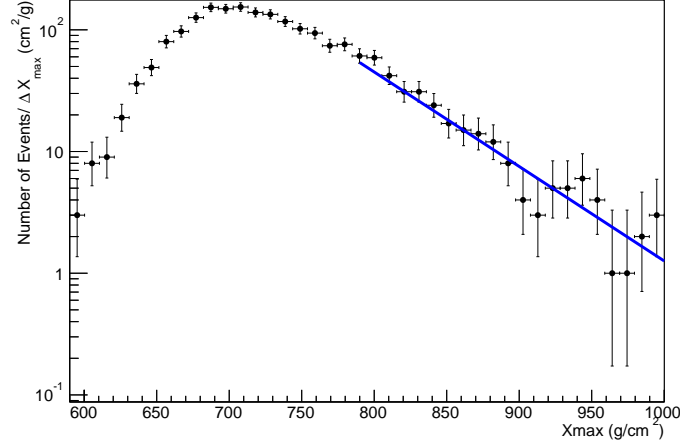


**Figure 2:** The number of events per  $X_{max}$  bin ( $\Delta X_{max}$ ) vs.  $X_{max}$   $g/cm^2$  for BRMLR fluorescence detector and the Telescope Array surface detector in hybrid mode. The line is the exponential fit to the slope using the unbinned likelihood method in 790-1000  $g/cm^2$  range.

including the statistical checks is found to be  $\Lambda_m = 55.9 \pm 3.8$  [Stat.]. Note that  $\Lambda_m$  is directly derived from the data and is model independent. Therefore, it can be used at a later time to calculate the inelastic proton-air cross section independently of the method or the UHECR models used in this paper.

## 2.2 Proton-Air cross Section Measurement

The inelastic proton-air cross section  $\sigma_{p-air}^{inel}$  is directly linked to the interaction mean free path of proton in air  $\lambda_{p-air}$  by the equation  $\sigma_{p-air} = \frac{\langle m_{air} \rangle}{\lambda_{p-air}}$ . Where  $\langle m_{air} \rangle$  is the mean target mass of air with the value of 24160 mb  $g\ cm^{-2}$ .

To determine the interaction mean free path of proton in air  $\lambda_{p-air}$  and therefore the inelastic proton-air cross section we use the  $K$ -Factor technique. Here, the exponential slope of the attenuation length is related to the hadronic interaction length by  $\Lambda_m = K\lambda_{p-air}$ . The  $K$  values are determined from the high energy models.

The calculation of the values of  $K$  is discussed in detail in [1] and [3]. The value of  $K$  is determined by measuring the ratio  $\Lambda_m/\lambda_{p-air}$  using a one-dimensional air shower Monte Carlo program CONEX 6.4 [11, 13, 25]. The  $K$  value is obtained for each high energy model QGSJETII.4 [24], QGSJET01 [21], SIBYLL2.3 [17], and EPOS-LHC [26] and the corresponding average value of the inelastic proton-air cross section including the statistical fluctuation is found to be  $\sigma_{p-air}^{inel} = 520.1 \pm 35.8$  [Stat.] mb.

A systematic uncertainty due to model dependence is reported. This done by quantifying the maximum variation in the  $\sigma_{p-air}^{inel}$  value for each model from the average  $\sigma_{p-air}^{inel}$  obtained from all the high energy models. This uncertainty was found to be equal to  $\pm 15$  mb.

The impact of contamination from other primaries is also considered. The systematic effect of other elements in the tail beside proton including photon, CNO, helium and iron is investigated.

Only photons and helium introduce a bias in the inelastic proton-air cross section.

The upper limit of cosmic-ray photon fraction at the energy range in this study is found to be  $\sim 1.0\%$ , which is the best upper limit in the Northern Hemisphere reported from the Yakutsk air-shower array [19]. The systematic uncertainty due to  $1.0\%$  gamma contamination is found to be  $+20$  mb.

A recent study done by the Telescope Array indicates that the contamination of helium between  $10^{18.2}$  and  $10^{19.0}$  eV is under  $43.8\%$ . Using this limit, the systematic uncertainty due to helium contamination is found to be  $-40$  mb.

The final proton-air cross section reported by the Telescope Array detector at an average energy of  $10^{18.45}$  eV using the *K*-Factor method and including the statistical and systematic checks is  $\sigma_{p\text{-air}}^{inel} = 520.1 \pm 35.8$  [Stat.]  $^{+25.3}_{-42.9}$  [Sys.] mb. This result is shown in Figure 3 and is compared to other experimental measurements and current high energy model predictions.

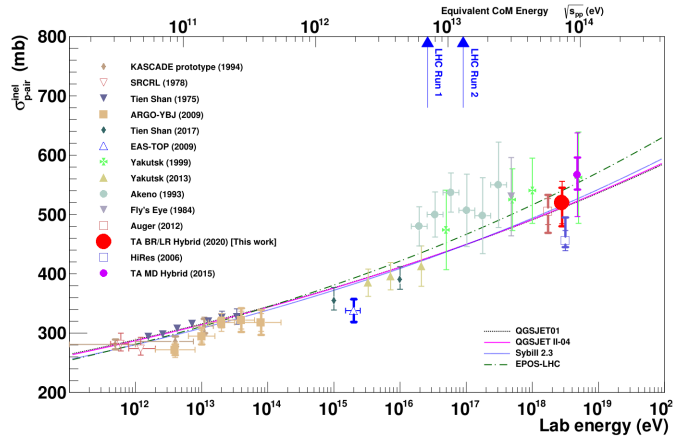


**Figure 3:** The proton-air cross section result of this work in comparison to previous experimental results [4–6, 9, 10, 20, 23, 27]. In addition, the high energy models (QGSJETII.4, QGSJET01, SIBYLL 2.3, EPOS-LHC) cross section predictions.

### 2.3 Proton-Proton Cross Section

The analysis to convert from the inelastic proton-air cross section to proton-proton cross section consist of two parts. The first part is done by converting the measured inelastic proton-air cross section to the possible allowed values of the proton-proton cross section in the  $(\sigma_{pp}^{tot}-B)$  plane, where  $\sigma_{pp}^{tot}$  is the total proton-proton cross section and B is the forward scattering elastic slope. The conversion is obtained using Glauber formalism [18]. The second part is done by calculating the intersection of the curves with one of the prediction models Block, Halzen, and Stanev (BHS) [12]. Note that the BHS model can be replaced with other models or predictions to solve for the  $\sigma_{pp}^{tot}$ . Note the BHS model is both consistent with the unitarity constraint while describing the pp and  $\bar{p}p$  cross section data from the Tevatron [14, 16].

The proton-proton cross section in this work is found to be  $\sigma_{pp}^{tot} = 139.4^{+23.4}_{-21.3}$  [Stat.]  $^{+15.7}_{-25.4}$ [Sys.] mb. This result is shown in Figure 4 in comparison to previously reported values by UHECR experiments [4, 9, 10, 20]. The recent result from LHC by TOTEM at  $\sqrt{s} = 7$  and 13 TeV [7, 8] is also shown, in addition to the BHS fit [12]. The best fit of the proton-proton total cross section data by the COMPETE collaboration is also added [15].

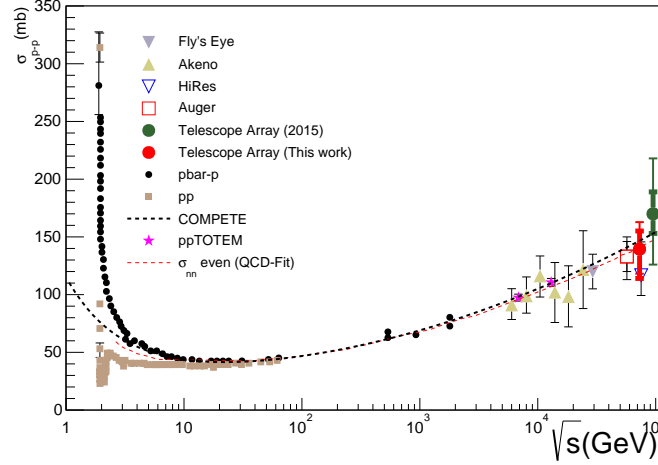


**Figure 4:** A compilation of the proton-proton cross section vs. the center of mass energy result of this work and previous work by cosmic rays detectors[ [1], [9], [20], [10], [4]]. The dashed red curve is the BHS fit [12] and the dashed black curve is the fit by the COMPETE collaboration citecompete. This plot is adapted and modified from [12].

### 3. Conclusion and Outlook

Telescope Array has measured the inelastic proton-air cross section of ultra high energy cosmic rays at  $\sqrt{s} = 73$  TeV. This measurement is performed for energies that are not accessible to accelerator experiments, therefore provides an important and unique test of standard model predictions about the fundamental nature of matter.

The Telescope Array utilizes a large array of surface detectors and fluorescence telescopes to record the atmospheric depth of maximum size of air showers initiated by inelastic collisions of ultra high energy cosmic rays and air molecules in the upper atmosphere. By combining the geometric and timing information of SDs and the Black Rock Mesa and Long Ridge FDs, the observe a hybrid event  $X_{max}$  can be determined with a good precision of  $\sim 20$  g/cm<sup>2</sup>. Using nearly nine years of hybrid data, TA measures  $\sigma_{p-air}^{inel} = 520.1 \pm 35.8$  [Stat.]  $^{+25.3}_{-42.9}$ [Sys.] mb for  $\sqrt{s} = 73$  TeV. Using Glauber theory and the Block, Halzen, Stanev model. The total proton-proton cross section is determined from  $\sigma_{p-air}^{inel}$  to be  $\sigma_{pp}^{tot} = 139.4^{+23.4}_{-21.3}$ [Stat.]  $^{+15.7}_{-25.4}$ [Sys.] mb.

Future cross section results, using TA×4 [22] will allow us to report on the proton air cross section with greater statistical power. Moreover, including data from the Telescope Array Lower

Extension [2] would allow the measurement in  $10^{17}$ – $10^{19}$  eV range with high statistical power and at several energy intervals. This would allow us to make a statement on the functional form of the cross section energy dependence.

## References

- [1] Abbasi, R. U. et al. (2015). Measurement of the proton-air cross section with Telescope Array's Middle Drum detector and surface array in hybrid mode. *Phys. Rev.*, D92(3):032007.
- [2] Abbasi, R. U. et al. (2018). The Cosmic-Ray Energy Spectrum between 2 PeV and 2 EeV Observed with the TALE detector in monocular mode. *Astrophys. J.*, 865(1):74.
- [3] Abbasi, R. U. et al. (2020). Measurement of the proton-air cross section with telescope array's black rock mesa and long ridge fluorescence detectors, and surface array in hybrid mode. *Phys. Rev. D*, 102:062004.
- [4] Abreu, P. et al. (2012). Measurement of the proton-air cross-section at  $\sqrt{s} = 57$  TeV with the Pierre Auger Observatory. *Phys.Rev.Lett.*, 109:062002.
- [5] Aglietta, M. and others (2009). Measurement of the proton-air inelastic cross section at  $\sqrt{s} \approx 2$  TeV from the EAS-TOP experiment. *Phys. Rev. D*, 79:032004.
- [6] Aielli, G. et al. (2009). Proton-air cross section measurement with the ARGO-YBJ cosmic ray experiment. *Phys.Rev.*, D80:092004.
- [7] Antchev, G. et al. (2011). First measurement of the total proton-proton cross section at the LHC energy of  $\sqrt{s} = 7$  TeV. *EPL*, 96(2):21002.
- [8] Antchev, G. et al. (2019). First measurement of elastic, inelastic and total cross-section at  $\sqrt{s} = 13$  TeV by TOTEM and overview of cross-section data at LHC energies. *Eur. Phys. J.*, C79(2):103.
- [9] Baltrusaitis, R., Cassidy, G., Elbert, J., Gerhardy, P., Ko, S., et al. (1984). Total Proton Proton Cross-Section at  $s^{(1/2)} = 30$ -TeV. *Phys.Rev.Lett.*, 52:1380–1383.
- [10] Belov, K. (2006). p-air cross-section measurement at  $10^{18.5}$ -eV. *Nucl.Phys.Proc.Suppl.*, 151:197–204.
- [11] Bergmann, T., Engel, R., Heck, D., Kalmykov, N., Ostapchenko, S., et al. (2007). One-dimensional Hybrid Approach to Extensive Air Shower Simulation. *Astropart.Phys.*, 26:420–432.
- [12] Block, M. and Halzen, F. (2005). New evidence for the saturation of the Froissart bound. *Phys.Rev.*, D72:036006.
- [13] Bossard, G. et al. (2001). Cosmic ray air shower characteristics in the framework of the parton-based gribov-regge model nexus. *Phys. Rev.*, D63:054030.

- [14] Buras, A. and Dias de Deus, J. (1974). Scaling law for the elastic differential cross-section in p p scattering from geometric scaling. *Nucl.Phys.*, B71:481–492.
- [15] Cudell, J. R. et al. (2002). Benchmarks for the forward observables at RHIC, the Tevatron Run II and the LHC. *Phys. Rev. Lett.*, 89:201801.
- [16] Dias De Deus, J. (1973). Geometric Scaling, Multiplicity Distributions and Cross-Sections. *Nucl.Phys.*, B59:231–236.
- [17] Fletcher, R., Gaisser, T., Lipari, P., and Stanev, T. (1994). SIBYLL: An Event generator for simulation of high-energy cosmic ray cascades. *Phys.Rev.*, D50:5710–5731.
- [18] Glauber, R. and Matthiae, G. (1970). High-energy scattering of protons by nuclei. *Nucl.Phys.*, B21:135–157.
- [19] Glushkov, A. et al. (2010). Constraints on the flux of primary cosmic-ray photons at energies  $E 10^{18}$  eV from Yakutsk muon data. *Phys. Rev. D*, 82:041101.
- [20] Honda, M. et al. (1993). Inelastic cross-section for p-air collisions from air shower experiment and total cross-section for p p collisions at SSC energy. *Phys.Rev.Lett.*, 70:525–528.
- [21] Kalmykov, N., Ostapchenko, S., and Pavlov, A. (1997). Quark-gluon string model and EAS simulation problems at ultra-high energies. *Nucl.Phys.Proc.Suppl.*, 52B:17–28.
- [22] Kido, E. (2019). Status and prospects of the TA<sub>x</sub>4 experiment. In *European Physical Journal Web of Conferences*, volume 210 of *European Physical Journal Web of Conferences*, page 06001.
- [23] Mielke, H., Foeller, M., Engler, J., and Knapp, J. (1994). Cosmic ray hadron flux at sea level up to 15-TeV. *J.Phys.*, G20:637–649.
- [24] Ostapchenko, S. (2006). QGSJET-II: Towards reliable description of very high energy hadronic interactions. *Nucl.Phys.Proc.Suppl.*, 151:143–146.
- [25] Pierog, T. et al. (2006). First results of fast one-dimensional hybrid simulation of eas using conex. *Nucl. Phys. Proc. Suppl.*, 151:159–162.
- [26] Pierog, T., Karpenko, I., Katzy, J., Yatsenko, E., and Werner, K. (2013). EPOS LHC : test of collective hadronization with LHC data.
- [27] Siohan, F., Ellsworth, R., Ito, A., Macfall, J., Streitmatter, R., et al. (1978). Unaccompanied Hadron Flux at a Depth of 730 –  $G/CM^2$ ,  $10^2$ -GeV  $< e < 10^4$ -GeV. *J.Phys.*, G4:1169–1186.

**Full Authors List: Telescope Array Collaboration**

R.U. Abbasi<sup>1</sup>, T. Abu-Zayyad<sup>1,2</sup>, M. Allen<sup>2</sup>, Y. Arai<sup>3</sup>, R. Arimura<sup>3</sup>, E. Barcikowski<sup>2</sup>, J.W. Belz<sup>2</sup>, D.R. Bergman<sup>2</sup>, S.A. Blake<sup>2</sup>, I. Buckland<sup>2</sup>, R. Cady<sup>2</sup>, B.G. Cheon<sup>4</sup>, J. Chiba<sup>5</sup>, M. Chikawa<sup>6</sup>, T. Fujii<sup>7</sup>, K. Fujisue<sup>6</sup>, K. Fujita<sup>3</sup>, R. Fujiwara<sup>3</sup>, M. Fukushima<sup>6</sup>, R. Fukushima<sup>3</sup>, G. Furlich<sup>2</sup>, R. Gonzalez<sup>2</sup>, W. Hanlon<sup>2</sup>, M. Hayashi<sup>8</sup>, N. Hayashida<sup>9</sup>, K. Hibino<sup>9</sup>, R. Higuchi<sup>6</sup>, K. Honda<sup>10</sup>, D. Ikeda<sup>9</sup>, T. Inadomi<sup>11</sup>, N. Inoue<sup>12</sup>, T. Ishii<sup>10</sup>, H. Ito<sup>13</sup>, D. Ivanov<sup>2</sup>, H. Iwakura<sup>11</sup>, A. Iwasaki<sup>3</sup>, H.M. Jeong<sup>14</sup>, S. Jeong<sup>14</sup>, C.C.H. Jui<sup>2</sup>, K. Kadota<sup>15</sup>, F. Kakimoto<sup>9</sup>, O. Kalashev<sup>16</sup>, K. Kasahara<sup>17</sup>, S. Kasami<sup>18</sup>, H. Kawai<sup>19</sup>, S. Kawakami<sup>3</sup>, S. Kawana<sup>12</sup>, K. Kawata<sup>6</sup>, I. Kharuk<sup>16</sup>, E. Kido<sup>13</sup>, H.B. Kim<sup>4</sup>, J.H. Kim<sup>2</sup>, J.H. Kim<sup>2</sup>, M.H. Kim<sup>14</sup>, S.W. Kim<sup>14</sup>, Y. Kimura<sup>3</sup>, S. Kishigami<sup>3</sup>, Y. Kubota<sup>11</sup>, S. Kurisu<sup>11</sup>, V. Kuzmin<sup>16\*</sup>, M. Kuznetsov<sup>16,20</sup>, Y.J. Kwon<sup>21</sup>, K.H. Lee<sup>14</sup>, B. Lubsandorzhiev<sup>16</sup>, J.P. Lundquist<sup>2,22</sup>, K. Machida<sup>10</sup>, H. Matsumiya<sup>3</sup>, T. Matsuyama<sup>3</sup>, J.N. Matthews<sup>2</sup>, R. Mayta<sup>3</sup>, M. Minamino<sup>3</sup>, K. Mukai<sup>10</sup>, I. Myers<sup>2</sup>, S. Nagataki<sup>13</sup>, K. Nakai<sup>3</sup>, R. Nakamura<sup>11</sup>, T. Nakamura<sup>23</sup>, T. Nakamura<sup>11</sup>, Y. Nakamura<sup>11</sup>, A. Nakazawa<sup>11</sup>, E. Nishio<sup>18</sup>, T. Nonaka<sup>6</sup>, H. Oda<sup>3</sup>, S. Ogio<sup>3,24</sup>, M. Ohnishi<sup>6</sup>, H. Ohoka<sup>6</sup>, Y. Oku<sup>18</sup>, T. Okuda<sup>25</sup>, Y. Omura<sup>3</sup>, M. Ono<sup>13</sup>, R. Onogi<sup>3</sup>, A. Oshima<sup>3</sup>, S. Ozawa<sup>26</sup>, I.H. Park<sup>14</sup>, M. Potts<sup>2</sup>, M.S. Pshirkov<sup>16,27</sup>, J. Remington<sup>2</sup>, D.C. Rodriguez<sup>2</sup>, G.I. Rubtsov<sup>16</sup>, D. Ryu<sup>28</sup>, H. Sagawa<sup>6</sup>, R. Sahara<sup>3</sup>, Y. Saito<sup>11</sup>, N. Sakaki<sup>6</sup>, T. Sako<sup>6</sup>, N. Sakurai<sup>3</sup>, K. Sano<sup>11</sup>, K. Sato<sup>3</sup>, T. Seki<sup>11</sup>, K. Sekino<sup>6</sup>, P.D. Shah<sup>2</sup>, Y. Shibasaki<sup>11</sup>, F. Shibata<sup>10</sup>, N. Shibata<sup>18</sup>, T. Shibata<sup>6</sup>, H. Shimodaira<sup>6</sup>, B.K. Shin<sup>28</sup>, H.S. Shin<sup>6</sup>, D. Shinto<sup>18</sup>, J.D. Smith<sup>2</sup>, P. Sokolsky<sup>2</sup>, N. Sone<sup>11</sup>, B.T. Stokes<sup>2</sup>, T.A. Stroman<sup>2</sup>, Y. Takagi<sup>3</sup>, Y. Takahashi<sup>3</sup>, M. Takamura<sup>5</sup>, M. Takeda<sup>6</sup>, R. Takeishi<sup>6</sup>, A. Taketa<sup>29</sup>, M. Takita<sup>6</sup>, Y. Tameda<sup>18</sup>, H. Tanaka<sup>3</sup>, K. Tanaka<sup>30</sup>, M. Tanaka<sup>31</sup>, Y. Tanoue<sup>3</sup>, S.B. Thomas<sup>2</sup>, G.B. Thomson<sup>2</sup>, P. Tinyakov<sup>16,20</sup>, I. Tkachev<sup>16</sup>, H. Tokuno<sup>32</sup>, T. Tomida<sup>11</sup>, S. Troitsky<sup>16</sup>, R. Tsuda<sup>3</sup>, Y. Tsunesada<sup>3,24</sup>, Y. Uchihori<sup>33</sup>, S. Udo<sup>9</sup>, T. Uehama<sup>11</sup>, F. Urban<sup>34</sup>, T. Wong<sup>2</sup>, K. Yada<sup>6</sup>, M. Yamamoto<sup>11</sup>, K. Yamazaki<sup>9</sup>, J. Yang<sup>35</sup>, K. Yashiro<sup>5</sup>, F. Yoshida<sup>18</sup>, Y. Yoshioka<sup>11</sup>, Y. Zhezher<sup>6,16</sup>, and Z. Zundel<sup>2</sup>

<sup>1</sup> Department of Physics, Loyola University Chicago, Chicago, Illinois, USA

<sup>2</sup> High Energy Astrophysics Institute and Department of Physics and Astronomy, University of Utah, Salt Lake City, Utah, USA

<sup>3</sup> Graduate School of Science, Osaka City University, Osaka, Osaka, Japan

<sup>4</sup> Department of Physics and The Research Institute of Natural Science, Hanyang University, Seongdong-gu, Seoul, Korea

<sup>5</sup> Department of Physics, Tokyo University of Science, Noda, Chiba, Japan

<sup>6</sup> Institute for Cosmic Ray Research, University of Tokyo, Kashiwa, Chiba, Japan

<sup>7</sup> The Hakubi Center for Advanced Research and Graduate School of Science, Kyoto University, Kitashirakawa-Oiwakecho, Sakyo-ku, Kyoto, Japan

<sup>8</sup> Information Engineering Graduate School of Science and Technology, Shinshu University, Nagano, Nagano, Japan

<sup>9</sup> Faculty of Engineering, Kanagawa University, Yokohama, Kanagawa, Japan

<sup>10</sup> Interdisciplinary Graduate School of Medicine and Engineering, University of Yamanashi, Kofu, Yamanashi, Japan

<sup>11</sup> Academic Assembly School of Science and Technology Institute of Engineering, Shinshu University, Nagano, Nagano, Japan

<sup>12</sup> The Graduate School of Science and Engineering, Saitama University, Saitama, Saitama, Japan

<sup>13</sup> Astrophysical Big Bang Laboratory, RIKEN, Wako, Saitama, Japan

<sup>14</sup> Department of Physics, SungKyunKwan University, Jang-an-gu, Suwon, Korea

<sup>15</sup> Department of Physics, Tokyo City University, Setagaya-ku, Tokyo, Japan

<sup>16</sup> Institute for Nuclear Research of the Russian Academy of Sciences, Moscow, Russia

<sup>17</sup> Faculty of Systems Engineering and Science, Shibaura Institute of Technology, Minato-ku, Tokyo, Japan

- <sup>18</sup> *Department of Engineering Science, Faculty of Engineering, Osaka Electro-Communication University, Neyagawashi, Osaka, Japan*
- <sup>19</sup> *Department of Physics, Chiba University, Chiba, Chiba, Japan*
- <sup>20</sup> *Service de Physique Théorique, Université Libre de Bruxelles, Brussels, Belgium*
- <sup>21</sup> *Department of Physics, Yonsei University, Seodaemun-gu, Seoul, Korea*
- <sup>22</sup> *Center for Astrophysics and Cosmology, University of Nova Gorica, Nova Gorica, Slovenia*
- <sup>23</sup> *Faculty of Science, Kochi University, Kochi, Kochi, Japan*
- <sup>24</sup> *Nambu Yoichiro Institute of Theoretical and Experimental Physics, Osaka City University, Osaka, Osaka, Japan*
- <sup>25</sup> *Department of Physical Sciences, Ritsumeikan University, Kusatsu, Shiga, Japan*
- <sup>26</sup> *Quantum ICT Advanced Development Center, National Institute for Information and Communications Technology, Koganei, Tokyo, Japan*
- <sup>27</sup> *Sternberg Astronomical Institute, Moscow M.V. Lomonosov State University, Moscow, Russia*
- <sup>28</sup> *Department of Physics, School of Natural Sciences, Ulsan National Institute of Science and Technology, UNIST-gil, Ulsan, Korea*
- <sup>29</sup> *Earthquake Research Institute, University of Tokyo, Bunkyo-ku, Tokyo, Japan*
- <sup>30</sup> *Graduate School of Information Sciences, Hiroshima City University, Hiroshima, Hiroshima, Japan*
- <sup>31</sup> *Institute of Particle and Nuclear Studies, KEK, Tsukuba, Ibaraki, Japan*
- <sup>32</sup> *Graduate School of Science and Engineering, Tokyo Institute of Technology, Meguro, Tokyo, Japan*
- <sup>33</sup> *Department of Research Planning and Promotion, Quantum Medical Science Directorate, National Institutes for Quantum and Radiological Science and Technology, Chiba, Chiba, Japan*
- <sup>34</sup> *CEICO, Institute of Physics, Czech Academy of Sciences, Prague, Czech Republic*
- <sup>35</sup> *Department of Physics and Institute for the Early Universe, Ewha Womans University, Seodaemun-gu, Seoul, Korea*

## Acknowledgements

The Telescope Array experiment is supported by the Japan Society for the Promotion of Science(JSPS) through Grants-in-Aid for Priority Area 431, for Specially Promoted Research JP21000002, for Scientific Research (S) JP19104006, for Specially Promoted Research JP15H05693, for Scientific Research (S) JP15H05741 and JP19H05607, for Science Research (A) JP18H03705, for Young Scientists (A) JPH26707011, and for Fostering Joint International Research (B) JP19KK0074, by the joint research program of the Institute for Cosmic Ray Research (ICRR), The University of Tokyo; by the Pioneering Program of RIKEN for the Evolution of Matter in the Universe (r-EMU); by the U.S. National Science Foundation awards PHY-1404495, PHY-1404502, PHY-1607727, PHY-1712517, PHY-1806797 and PHY-2012934; by the National Research Foundation of Korea (2017K1A4A3015188, 2020R1A2C1008230, & 2020R1A2C2102800) ; by the Ministry of Science and Higher Education of the Russian Federation under the contract 075-15-2020-778, RFBR grant 20-02-00625a (INR), IISN project No. 4.4501.18, and Belgian Science Policy under IUAP VII/37 (ULB). This work was partially supported by the grants of The joint research program of the Institute for Space-Earth Environmental Research, Nagoya University and Inter-University Research Program of the Institute for Cosmic Ray Research of University of Tokyo. The foundations of Dr. Ezekiel R. and Edna Wattis Dumke, Willard L. Eccles, and George S. and Dolores Doré Eccles all helped with generous donations. The State of Utah supported the project through its Economic Development Board, and the University of Utah through the Office of the Vice President for Research. The experimental site became available through the cooperation of the Utah School

---

\* Deceased

and Institutional Trust Lands Administration (SITLA), U.S. Bureau of Land Management (BLM), and the U.S. Air Force. We appreciate the assistance of the State of Utah and Fillmore offices of the BLM in crafting the Plan of Development for the site. Patrick A. Shea assisted the collaboration with valuable advice and supported the collaboration's efforts. The people and the officials of Millard County, Utah have been a source of steadfast and warm support for our work which we greatly appreciate. We are indebted to the Millard County Road Department for their efforts to maintain and clear the roads which get us to our sites. We gratefully acknowledge the contribution from the technical staffs of our home institutions. An allocation of computer time from the Center for High Performance Computing at the University of Utah is gratefully acknowledged.